ACS chemical biology

ARTICLES

pubs.acs.org/acschemicalbiology

Ca^{2+} Homeostasis Modulation Enhances the Amenability of L444P Glucosylcerebrosidase to Proteostasis Regulation in Patient-Derived Fibroblasts

Fan Wang,[†] Giulia Agnello,[†] Natasha Sotolongo,[‡] and Laura Segatori[†,‡,*]

[†]Department of Chemical and Biomolecular Engineering and [‡]Department of Biochemistry and Cell Biology, Rice University, CHBE-MS 362, 6100 Main St., Houston, Texas 77005, United States

Supporting Information

ABSTRACT: Gaucher's disease is caused by deficiency of lysosomal glucocerebrosidase (GC) activity and accumulation of GC substrate, glucosylceramide. A number of point mutations in GC encoding gene have been reported to destabilize the enzyme native structure, resulting in protein misfolding and degradation. Particularly, the L444P GC variant, often associated with neuropathic manifestations of the disease, is severely destabilized and immediately degraded, resulting in complete loss of enzymatic activity. In addition, glucosylceramide accumulation causes Ca^{2+} efflux from the endoplasmic reticulum (ER) through ryanodine receptors (RyRs) in the neurons of Gaucher's disease patients. We hypothesized that excessive $[Ca^{2+}]_{ER}$ efflux impairs ER folding and studied how modulation of $[Ca^{2+}]_{ER}$ affects folding of L444P GC in patient-derived fibroblasts. We report that RyRs blockers mediated $[Ca^{2+}]$ modulation, recreating a "wild type-like" folding environment in the ER, more amenable to rescuing the folding of mutated L444P GC through proteostasis regulation. Treating patient-derived fibroblasts with a RyRs blocker and a proteostasis modulator, MG-132, results in enhanced folding, trafficking, and activity of the severely destabilized L444P GC variant. Global gene expression profiling and mechanistic studies were conducted to investigate the folding quality control expression pattern conducive to native folding of mutated L444P GC and revealed that the ER-lumenal BiP/GRP78 plays a key role in the biogenesis of this GC variant.

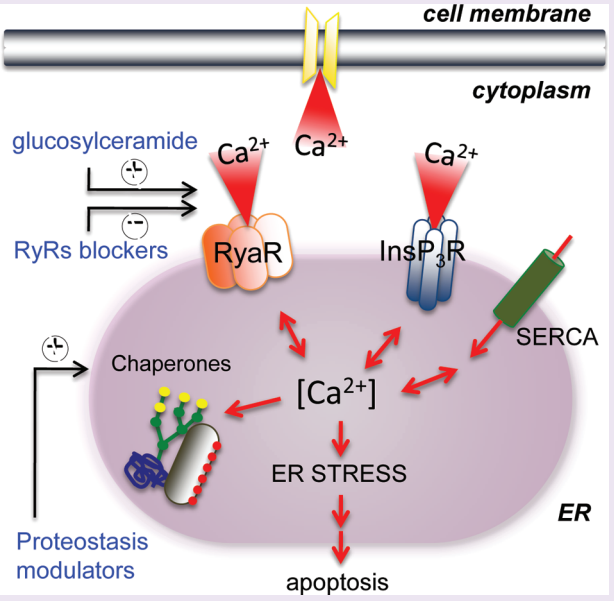

Lysosomal storage disorders (LSDs) include more than 40 clinically distinct genetic diseases characterized by lysosomal accumulation of metabolites such as lipids and glycoproteins.[1] Although leading to a range of different clinical manifestations, the pathogenesis of most LSD is caused by loss of the disease-associated enzyme due to inactivating or misfolding mutations and failure of the enzyme to reach the lysosomes, leading to loss of a specific lysosomal hydrolytic activity and consequently substrate accumulation.[1]

Gaucher's Disease (GD), the most common among LSD, is caused by mutations in the gene (GBA, NM_000157.2) encoding glucocerebrosidase (GC) and lysosomal accumulation of GC substrate, glucosylceramide.[2] GC is a 497-residue membrane-associated lysosomal glycoprotein. A number of mutations have been characterized.[3] Nonsense mutations have been identified[3] that directly inactivate the enzyme activity. However, a number of catalytically active GC variants contain missense mutations that destabilize GC native structure, compromising its folding[4] and leading to its retrotranslocation to the cytoplasm for endoplasmic reticulum (ER)-associated degradation (ERAD)[4,5] The main currently adopted treatment, enzyme replacement therapy,[6] is of limited efficacy[7,8] and is completely inadequate for treatment of neuropathic symptoms as a result of the inability of the injected protein to cross the blood brain barrier. Substrate reduction therapy[9] is rarely used as an alternative to enzyme replacement therapy because of the numerous associated side effects. Therapeutic solutions for neuropathic GD, as well as for a number of other neuropathic LSDs, are clearly an urgent medical need.

L444P is one of the most common among GC mutations, always associated with neuropathic symptoms in homozygous

Received: August 18, 2010
Accepted: November 2, 2010
Published: November 2, 2010

patients.[10] L444 is located in the hydrophobic core of a domain structurally distinct from the enzyme catalytic domain. The L444P substitution most likely causes a local conformational change that disrupts the domain's hydrophobic core and leads to the domain misfolding. As a result, the interaction of L444P GC with saposin C, GC activator, and acidic phospholipids is impaired, leading to complete loss of GC activity and severe neuronopathic symptoms.[11,12]

Chemical chaperones, small molecules structurally similar to the enzyme active site inhibitor, were recently demonstrated to stabilize the native structure of mutated GC variants and chaperone them to the lysosome,[13] thereby rescuing folding and activity. Interestingly, chemical chaperones were proven to rescue the folding of several GC variants containing mutations in the active site domain but failed to rescue L444P GC folding,[14] suggesting that the domain containing position 444 folds independently from the active site domain and is not stabilized by the interaction of chemical chaperones with the enzyme catalytic domain.

A number of LSD-associated enzyme variants containing missense mutations retain catalytic activity if forced to fold into their native structure. L444P GC folding is rescued to 50% of the wild type enzyme activity, which is compatible with effective treatment,[2] in patient-derived fibroblasts cultured at suboptimal temperatures,[13] a stress-inducing treatment that leads to enhancement of the cellular folding capacity. This approach was recently recapitulated using small molecules that modulate the composition of the proteostasis network.[15] Particularly, by influencing general cellular folding pathways, proteostasis regulators promote folding of unstable ER substrates. Owing to their non-substrate-specific mechanisms, they were shown to restore the activity of different enzymes associated with distinct LSD.[16]

Loss of GC activity has been repeatedly studied in patient-derived skin fibroblasts.[17] The cellular accumulation and enzymatic activity of GC variants in skin fibroblasts are used as an indication of the severity of GD manifestation and whether it is associated with neuropathic symptoms.[18,19] Moreover, patient-derived fibroblasts are specifically used for diagnostic purposes because residual activity of mutated GC variants is related to the clinical severity of the disease.[20,21] Thus, patient-derived fibroblasts carrying L444P GC were used in this study to investigate strategies to rescue the folding of the severely destabilized L444P GC variant, normally associated with complete loss of residual activity and manifestation of GD with neuropathic symptoms.

Ca^{2+} homeostasis plays a fundamental role in the biogenesis of secretory proteins as the activities of a number of ER chaperones including BiP/GRP78, Calnexin (CNX), and Calreticulin (CRT) are influenced by fluctuations in $[Ca^{2+}]_{ER}$,[22] which is highly regulated through Ca^{2+} release and uptake mechanisms. Ca^{2+} is released from the ER through ryanodine receptors (RyRs) or inositol 1,4,5-trisphosphate (IP3) receptors and pumped into the ER by Ca^{2+}-ATPases (SERCA pumps).[23] In GD cells, the accumulation of GC substrate, glucosylceramide, causes excessive $[Ca^{2+}]_{ER}$ release, specifically via RyRs.[24−26] We speculated that by affecting ER Ca^{2+} mobilization, glucosylceramide accumulation impairs ER folding and possibly further hampers the folding of unstable GC variants. Interestingly, impairment of Ca^{2+} homeostasis is a common theme in LSD, as substrate accumulation causes lowered $[Ca^{2+}]_{ER}$ in Sandhoff[27] and Niemann-Pick type A disease[28] and lysosomal $[Ca^{2+}]$ reduction in Niemann-Pick type C1 disease.[29] Recently, Ong *et al.* used patient-derived fibroblasts harboring the L444P GC variant to investigate impairment of Ca^{2+} homeostasis in GD and reported that $[Ca^{2+}]_{ER}$ can be restored by reducing $[Ca^{2+}]_{ER}$ efflux through the RyRs.[30]

On the basis of the notions that (i) $[Ca^{2+}]_{ER}$ affects ER chaperone expression and activity[22] and (ii) mutated GC folding is rescued by enhancement of the innate cellular folding capacity,[13] we hypothesized that the folding of LSD-associated enzymes could be restored by inhibiting $[Ca^{2+}]_{ER}$ depletion. We used L444P GC patient-derived fibroblasts to investigate the effect of $[Ca^{2+}]_{ER}$ modulation on the folding, trafficking, and activity of this mutated GC variant. We demonstrated that modulation of $[Ca^{2+}]_{ER}$ through inhibition of RyRs in L444P GC fibroblasts, although not directly promoting considerable rescue of L444P GC folding, reinstates a "wild type-like" ER environment, more amenable to proteostasis regulation, particularly through upregulation of the ER chaperone BiP. We also profiled global gene expression of cells treated with a RyRs blocker and a proteostasis modulator, MG-132, and report mechanistic studies validating the influence of selected ER chaperones, particularly BiP, on L444P GC folding.

RESULTS AND DISCUSSION

The purpose of this study was to investigate modulation of Ca^{2+} homeostasis through small molecule Ca^{2+} receptor blockers in GD patient-derived fibroblasts. Counteracting the effect of glucosylceramide accumulation on $[Ca^{2+}]_{ER}$ depletion is suggested as a strategy to restore ER Ca^{2+} homeostasis, which is known to be intimately associated with the function of the ER chaperone machinery. To explore this approach we also combined it with cell treatment with a small molecule proteostasis regulator that upregulates the innate cellular folding capacity, MG-132.[16] Modulation of $[Ca^{2+}]_{ER}$ is suggested as a strategy to restore the ER folding capacity, while proteostasis regulation is ursued as a means to enhance it. Moreover, genetic engineering and cell treatment with small molecule Ca^{2+} homeostasis and proteostasis regulators were used to investigate changes in the expression of folding quality control genes that directly influence the folding of GC and to modulate the expression of ER chaperones to identify specific proteins of the ER folding pathway that rescue the folding of L444P GC.

Inhibition of $[Ca^{2+}]_{ER}$ Depletion Enhances MG-132 Function As a Proteostasis Regulator in L444P GC Patient-Derived Fibroblasts. Patient-derived fibroblasts harboring L444P GC were treated with small molecules RyRs blockers, including ryanodine,[31,32] dantrolene,[33] ruthenium red,[31] and 1,1′-diheptyl-4,4′-bipyridinium (DHBP) dibromide,[31,34] and GC activity was evaluated with the intact cell GC activity assay.[14] L444P GC activity was observed to increase up to 1.3-fold in cells treated with ryanodine (10−20 μM final medium concentration) for 48 h and decrease with increasing time of incubation (Figure S1a in Supporting Information). Although this modest increase in GC activity is expected to ameliorate GD symptoms,[2] we attempted enhancing ryanodine-mediated L444P GC folding by combining ryanodine with a proteostasis regulator, MG-132, which is known to rescue L444P GC folding through a mechanism distinct from $[Ca^{2+}]_{ER}$ modulation.[16] Co-administration of ryanodine (20 μM) and MG-132 (0.4 μM) for 72 h resulted in a 2.6-fold increase ($p < 0.001$) in L444P GC activity compared to untreated cells, which is higher than that observed using ryanodine (1.1-fold) or MG-132 (2.1-fold) under the same conditions (Figure 1a). We hypothesized that ryanodine

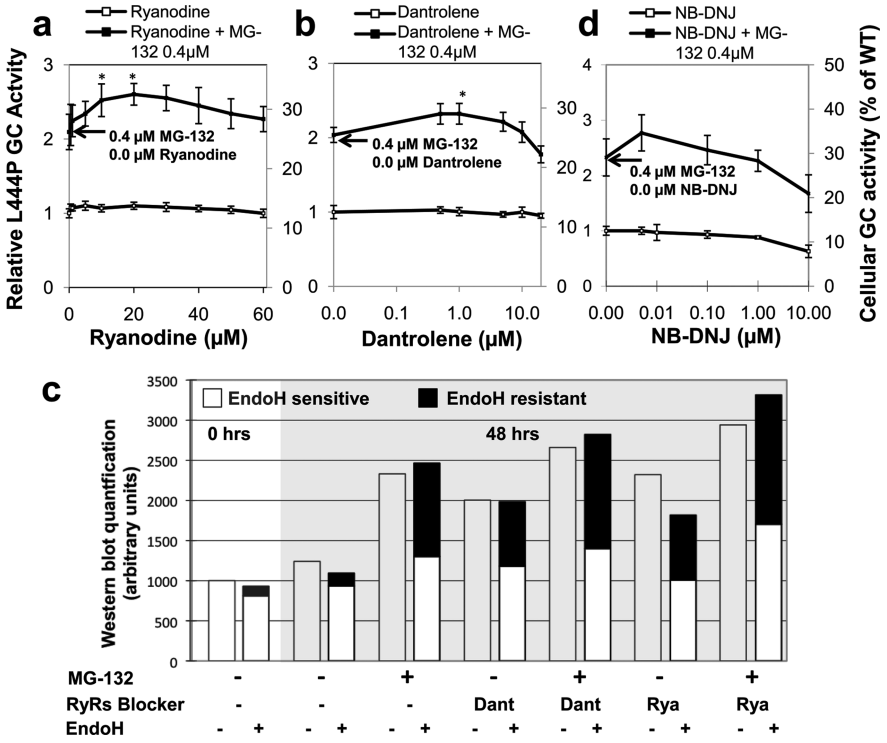

Figure 1. L444P GC folding, lysosomal trafficking and activity of patient-derived fibroblasts treated with RyRs blockers or glucosylceramide inhibitor and MG-132. Relative L444P GC activities of cells treated with (a) ryanodine and MG-132, (b) dantrolene and MG-132, and (d) NB-DNJ and MG-132. GC activities were obtained normalizing the activities measured in treated cells by the activity of untreated cells (left *y* axis), ($p < 0.01$ if not specified; $^*p < 0.001$). The corresponding fraction of WT GC activity is reported (right *y* axis). Experiments were repeated three times; data points were reported as mean ± SD. (c) Lysosomal trafficking of L444P GC in cells treated with ryanodine (20 μM), dantrolene (1 μM), and MG-132 (0.4 μM). EndoH treated and untreated samples were analyzed by Western blot. Quantification of EndoH-sensitive bands (ER retained GC) is reported in the white portion of the bars, and that of EndoH-resistant bands (lysosomal GC) is reported in the black top portions. Band analyses and quantifications were conducted using NIH Java Image analysis software.

partially or completely restores Ca^{2+} homeostasis, reestablishing a "wild type-like" folding environment in the ER of L444P GC fibroblasts that is normally characterized by substrate accumulation-induced Ca^{2+} efflux and thus impaired folding. Restoring a "wild type-like" ER environment is not sufficient to considerably enhance the folding of L444P GC, a severely destabilized enzyme variant normally immediately targeted to ERAD. However, by preventing $[Ca^{2+}]_{ER}$ depletion, ryanodine treatment renders L444P GC cells more amenable to protestasis regulation via MG-132.

Among the RyRs blockers tested, dantrolene was also observed to enhance MG-132-induced L444P GC activity increase. Co-administration of dantrolene (1 μM) and MG-132 (0.4 μM) resulted in 2.1-, 2.3-, and 2.5-fold increase in L444P GC activity after 48, 72, and 96 h of incubation, respectively (Figure 2b and Figure S1b in Supporting Information). Ruthenium red and DHBP were observed to marginally influence L444P GC activity and were not used in further studies due to their highly cytotoxic effect (data not shown).

To confirm that the detected increase in GC activity is caused by partial restoration of L444P GC folding and trafficking, its glycosylation state was evaluated with endoglycosidase H (EndoH). EndoH hydrolyzes high mannose but not mature N-glycan complexes, and thus GC detection by Western blot analysis of EndoH treated proteins reveals a low MW band corresponding to partially glycosylated, ER-retained GC (EndoH-sensitive) and a high MW band corresponding to fully glycosylated lysosomal GC (EndoH-resistant).[35] The total protein content of cells cultured with ryanodine (20 μM), dantrolene (1 μM), MG-132 (0.4 μM), or a combination thereof (Figure 1c) was subjected to EndoH treatment, and GC was detected by Western blot (Figure S1c in Supporting Information). In untreated cells 90% of L444P GC was EndoH-sensitive, and total GC amount and glycosylation state did not change with cell growth (Figure 1c). Dantrolene or ryanodine treatment resulted in a 1.6- and 1.9-fold increase in total L444P GC, respectively, and a decrease of EndoH-sensitive fraction to 60% of total GC. MG-132 treatment resulted in an increase of total and EndoH-resistant L444P GC, as previously reported.[16] In cells treated with MG-132 and ryanodine or dantrolene (corresponding to 2.5- and2.1-fold activity increase, respectively), the total GC content increased 2.4- and 2.1-fold, respectively, and nearly 50% of L444P GC was present in the EndoH-resistant form (Figure 1c).

Because glucosylceramide accumulation causes $[Ca^{2+}]_{ER}$ depletion, we hypothesized that inhibition of glucosylceramide synthesis would provide an alternative mechanism to RyRs inhibition to prevent abnormal $[Ca^{2+}]_{ER}$ efflux. Inhibition of glucosylceramide synthesis was investigated using N-butyl-deoxynojirimycin (NB-DNJ)[36] and MG-132. A barely detectable increase in L444P GC activity was observed in patient-derived fibroblasts cultured with NB-DNJ for up to 192 h and assayed every 24hrs. However, coadministration of NB-DNJ (5 nM) and MG-132 (0.4 μM) resulted in 2.8-fold increase in L444P GC activity ($p < 0.01$), higher than the 2.3-fold increase ob tained with MG-132 alone (Figure 1d), demonstrating that

dx.doi.org/10.1021/cb100321m |*ACS Chem. Biol.* 2011, 6, 158–168

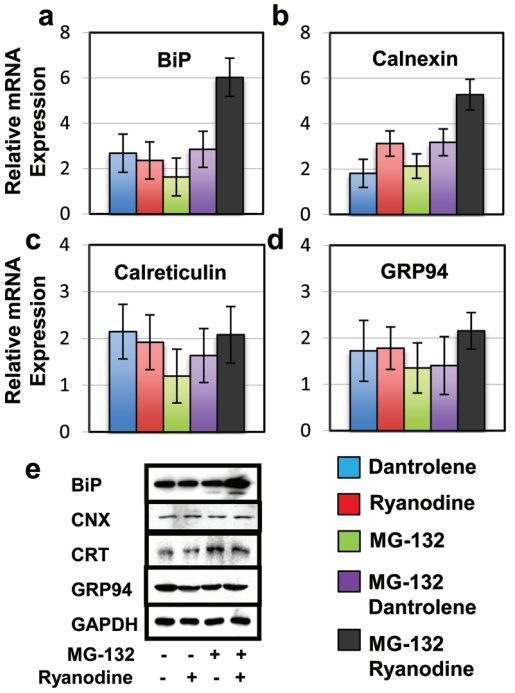

Figure 2. Expression of representative ER chaperones in L444P GC patient-derived fibroblasts treated with RyRs blockers and MG-132. Relative mRNA expression of ER chaperones: (a) BiP ($p < 0.01$), (b) CNX ($p < 0.01$), (c) CRT ($p < 0.05$), and (d) GRP94 ($p < 0.05$) evaluated by quantitative RT-PCR in L444P GC fibroblasts treated with ryanodine (20 μM), dantrolene (1 μM), and MG-132 (0.4 μM) for 24 h. mRNA expression levels of treated cells were corrected for the expression of the housekeeping gene GAPDH and normalized to those of untreated cells. The data is reported as mean ± SD. (e) Western blot analyses of representative ER chaperones in cells treated with ryanodine (20 μM) and MG-132 (0.4 μM) for 48 h. GAPDH expression is used as loading control.

glucosylceramide synthesis inhibition recapitulates the effect of RyRs blockers on L444P GC folding.

The results reported in Figure 1, taken together, demonstrate that inhibiting glucosylceramide-induced $[Ca^{2+}]_{ER}$ depletion via RyRs enhances MG-132 ability to restore L444P GC proteostasis. Simply preventing $[Ca^{2+}]_{ER}$ efflux through RyRs or glucosylceramide synthesis inhibition only modestly increased L444P GC activity. In agreement with this finding, expression of L444P GC in wild type fibroblasts has been shown not to rescue L444P GC folding,[5] suggesting that the innate (wild type) folding capacity cannot cope with the destabilizing effect of the L444P substitution. However, restoring a "wild type-like" folding environment in the ER of GD cells harboring L444P GC via RyRs or glucosylceramide synthesis inhibition enhances MG-132-mediated L444P GC proteostasis.

Ong *et al.* recently reported a study on $[Ca^{2+}]_{ER}$ modulation induced rescue of mutated GC folding.[30] In this study, siRNA knockdown of RyRs and treatment of GD fibroblasts with RyRs inhibitors was reported to modestly increase the pool of L444P GC that escapes ERAD and restore L444P GC activity measured with lysed cell GC activity assay (particularly dantrolene 25 μM, 1.3-fold), in agreement with what is reported here using dantrolene and ryanodine (Figure 1). However, dantrolene (10 μM) treatment was reported to lower L444P GC activity, despite increasing the pool of EndoH-resistant glycosylated L444P GC that traffics to the lysosome, implying that in cells treated with dantrolene L444P GC is natively folded but is not enzymatically active. This was attributed to L444P GC hypersensitivity inhibition,[30] supported by the lowered L444P GC activity rescue observed in cells treated with MG-132 (0.25 μM) and dantrolene (10 μM) compared to that in cells treated with MG-132 alone and by dantrolene's (10−300 μM) inhibitory effect on wild type GC *in vitro*. We hypothesize that the lowered L444P GC activity observed in cells treated with MG-132 and dantrolene is due to the high dantrolene concentration and long incubation times used, which in our hands were observed to give rise to cell toxicity and thus avoided. Furthermore, we suggest that chemical chaperones, whose mechanism is based on stabilization of the native enzyme structure mediated by binding to the enzyme active site, can have an inhibitory effect on the folding of L444P GC.[26] This is likely due to the fact that the L444P substitution is located in an independently folding domain (distinct from the active-site domain[37]) that is not stabilized by the interaction of chemical chaperones with L444P GC active site. However, this inhibitory effect[14] is not likely to apply to proteostasis regulators, including MG-132, or small molecules, such as RyRs inhibitors, that do not directly bind to GC intermediates.

BiP Expression Is Upregulated in L444P GC Patient-Derived Fibroblasts Treated with Ryanodine and MG-132. Cells treated with MG-132 and ryanodine partially restore L444P GC activity to 33% of wild type GC, compatible with effective treatment.[2] Thus, RyRs blockers and MG-132 were used to identify transcriptional changes potentially associated with the rescue of L444P GC folding, which were in turn investigated to validate their influence on mutated GC folding.

Quantitative RT-PCR of representative ER chaperones was used to investigate the influence of RyRs blockers and MG-132 on the ER folding machinery.[38] L444P GC cells were incubated with MG-132 (0.4 μM), dantrolene (1 μM), ryanodine (20 μM), or a combination thereof (Figure 2), and relative mRNA expression levels of BiP, Calnexin (CNX), Calreticulin (CRT), and GRP94 were evaluated. BiP expression was increased by ryanodine treatment (2.4-fold), and ryanodine and MG-132 cotreatment (6.0-fold). Similar results were obtained with dantrolene (2.7-fold) and dantrolene and MG-132 (2.9-fold) (Figure 2a). The difference in ryanodine- and dantrolene-mediated BiP upregulation might result from their binding to distinct sites of RyRs.[39] Analogous results were observed for CNX expression upon ryanodine (3.1-fold), and ryanodine and MG-132 (5.3-fold) treatment, or dantrolene (1.8-fold) and dantrolene and MG-132 (3.2-fold) treatment (Figure 2b). CRT and GRP94 expression were not considerably altered (Figure 2c and d).

ER chaperone protein concentrations were also evaluated by Western blot in cells treated with ryanodine and MG-132 (Figure 2e). BiP protein accumulation was enhanced by cotreatment with ryanodine and MG-132 compared to untreated cells or cells treated with either molecule, but we failed to observe significant changes in CNX, CRT, and GRP94 protein levels. These results are consistent with RT-PCR analyses, with the exception of CNX expression, for which the transcriptional increase is not reflected at the translational level, suggesting that CNX upregulation induced by cell treatment with MG-132 and ryanodine does not translate into enhanced accumulation of CNX protein.

Proteostasis Regulation and Modulation of Ca^{2+} Homeostasis Alters Global Gene Expression in L444P GC Patient-Derived Fibroblasts. Global gene expression was evaluated as

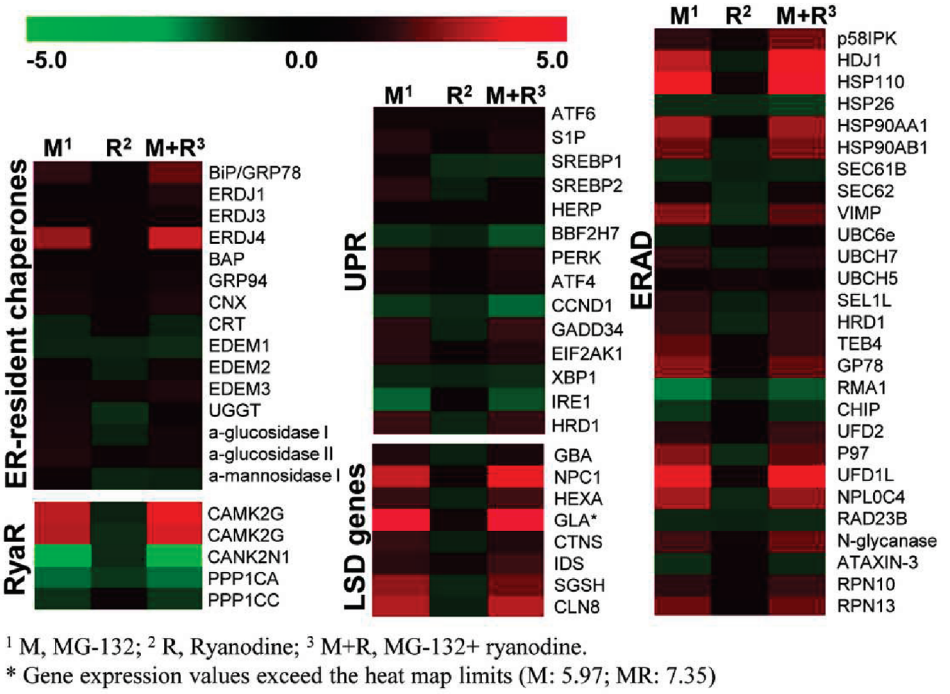

[1] M, MG-132; [2] R, Ryanodine; [3] M+R, MG-132+ ryanodine.
* Gene expression values exceed the heat map limits (M: 5.97; MR: 7.35)

Figure 3. Profiling of gene expression in L444P GC patient-derived fibroblasts treated with MG-132 and ryanodine. Transcriptional modulation of genes encoding for ER-resident chaperones and associated with UPR, LSD, lipid metabolism, and ERAD in L444P GC fibroblasts untreated and treated with MG-132 (0.4 μM) and ryanodine (20 μM). The expression of representative genes is reported as a heat map ($p < 0.01$); colors in the heat map represent deviation from the average control phenotype: green, lower activity; red, higher activity.

described in Methods in cells treated with MG-132 (0.4 μM), ryanodine (20 μM), and both MG-132 and ryanodine, for 24 h (Figure 3) and is reported as fold-change relative to untreated cells ($p < 0.01$, Table S2 in Supporting Information).

Among ER chaperones, BiP was found to be upregulated by MG-132 (1.8-fold increase), not considerably affected by ryanodine, but further upregulated by cotreatment with both MG-132 and ryanodine (2.3-fold), suggesting a direct correlation between MG-132 and ryanodine cotreatment-induced BiP upregulation and L444P GC activity rescue. Other ER chaperones and cochaperones were found to be modestly upregulated by MG-132 and ryanodine. Interestingly, even though ryanodine treatment barely altered their expression, in most cases it seemed to facilitate MG-132 folding-promoting function, as it enhanced ER folding and attenuated ERAD induced by MG-132 (see enhanced upregulation of CNX and EDEM3 and lowered upregulation of α-glucosidase II, Table S2 in Supporting Information).

The unfolded protein response (UPR), a complex tripartite pathway activated by excessive load of unfolded and misfolded proteins in the ER,[40] was also analyzed and found to be influenced by MG-132, but only marginally by ryanodine treatment. As part of the first UPR branch, double-stranded RNA-activated ER kinase (PERK[41]) activation induces phosphorylation of the translation initiation factor-2α (eIF2α), which results in lowered translation initiation. PERK and eIF2α were upregulated by MG-132 (1.5- and 1.4-fold, respectively). When ER proteostasis is restored, PERK is quickly dephosphorylated by GADD34, for which expression was also found to be upregulated (1.7-fold, MG-132; 1.9-fold, MG-132 and ryanodine). This arm of the UPR seems to be both upregulated and inhibited, suggesting activation of simultaneous cycles of moderate UPR activation and inhibition in treated cells. The second UPR branch involves upregulation of ER chaperones and ERAD for enhanced ER protein processing capacity. Again, the expression of UPR activators IRE1, XBP1, and ATF6[42] and their effector genes[43] were found to be both upregulated and inhibited by small molecule treatment (Table S2 in Supporting Information). The third branch of the UPR is activated when proteostasis cannot be re-established and culminates with BAX- and BAK-mediated apoptosis induction.[44] MG-132-induced BAK upregulation (1.7-fold) suggests that MG-132 acts by inducing a specific pro-apoptotic machinery. IRE1 also contributes to cell death through Jun N-terminal kinase (JNK)-mediated inactivation of the anti-apoptotic regulator BCL-2.[45] Interestingly, although BCL-2 is downregulated 6.2-fold by MG-132, ryanodine attenuates MG-132 downregulation (5-fold), suggesting that restoring Ca^{2+} homeostasis through RyRs inhibition has an anti-apoptotic effect in GD cells.

LSD-associated genes were found to be upregulated by MG-132 and MG-132 and ryanodine cotreatment (Table S2 in Supporting Information). Specifically, genes associated with Gaucher's, Niemann-Pick, Tay-Sachs, and Fabry diseases were upregulated by MG-132 (1.5-, 3.4-, 1.9-, and 6.0-fold, respectively) and MG-132 and ryanodine (1.4-, 3.9-, 2.0-, and 7.3-fold). MG-132- and ryanodine-induced increase in L444P GC expression was confirmed at the protein level by Western blot analyses (Figure S2 in Supporting Information). UPR activation is known to enhance lipid metabolism to increase the size of the ER and dilute the load of misfolded proteins.[42] Because LSD-associated proteins are enzymes normally involved in lipid degradation, we suggest that LSD genes' upregulation in L444P GC cells treated with MG-132 and ryanodine is a response of the cell to MG-132-induced UPR activation. L444P GC and other LSD-associated enzyme variants are

normally targeted to ERAD, and thus we suggest that increasing the concentration of newly synthesized enzyme through small molecule treatment could be a particularly appealing therapeutic strategy as it inevitably increases the pool of ER intermediates amenable to folding rescue. This MG-132-induced effect on L444P GC expression also explains the previously reported L444P GC folding increase observed treating GD cells with MG-132 and a chemical chaperone (N-(n-nonyl)-deoxynojirimycin, NN-DNJ).[16] L444P GC was initially shown not to be amenable to chemical chaperoning,[14] for which the mechanism, as mentioned above, is based on active site binding-mediated stabilization of the native enzyme structure, and most likely does not affect the independently folding domain containing the L444P substitution.[37] A dramatic increase in L444P GC activity was demonstrated by subjecting MG-132-treated L444P GC patient-derived cells to brief, temporally spaced pulses of low concentration NN-DNJ treatment. Such dosing schedule was devised to promote MG-132-mediated enhancement of the folded L444P GC pool that can be chaperoned by NN-DNJ through the secretory pathway.[16] MG-132-induced L444P GC upregulation provides a complementary explanation to the synergic effect of MG-132 and NN-DNJ on L444P GC folding. Although additional experiments are required to investigate this speculation, we suggest that GC upregulation, even that of the mutated variant, could be exploited to enhance mutated GC folding rescue by combining it with BiP expression induction and other proteostasis modulation based strategies.

ERAD is induced by UPR activation to lower the accumulation of misfolded proteins.[46] ER and cytoplasmic chaperones sense the accumulation of misfolded soluble and membrane protein, respectively. As mentioned above, among ER chaperones BiP was upregulated by cell treatment with MG-132 and ryanodine. Several cytoplasmic chaperones were dramatically upregulated (see Hsp70: 24.7-fold, MG-132; 33.0-fold, MG-132 and ryanodine). Substrate recognition is coupled with delivery of misfolded substrates to the retrotranslocation channel, ubiquination, and proteasomal degradation, steps involving a number of genes that were found to be mildly upregulated by MG-132 and not particularly affected by ryanodine treatment (Table S2 in Supporting Information).

MG-132 and ryanodine treatment also influenced the activity of RyRs. RyRs are inactivated by Ca^{2+}/calmodulin-dependent protein kinase II (CAMK2) phosphorylation,[47] an effect reversed by phosphatase PPP1C and by CAMK2 inhibitor (CAMK2N1). CAMK2 δ and γ subunits were upregulated by MG-132 (1.5- and 3.3-fold) and by MG-132 and ryanodine (1.6 and 3.8-fold), whereas CAMK2 inhibitor and PPP1C were greatly downregulated (CAMK2N1: 4.0-fold decrease, MG-132; 5.9-fold decrease, MG-132 and ryanodine; PPP1C α subunit: 1.9-fold decrease, MG-132).

Plasmid-Induced BiP Overexpression and Chromosomal BiP Upregulation Enhance MG-132 Function As a Proteostasis Regulator in L444P GC Patient-Derived Fibroblasts. In order to test whether ryanodine and MG-132-induced ER chaperone upregulation directly influences L444P GC folding, we attempted overexpressing the genes of interest in GD cells. Patient-derived fibroblasts were transfected with tetracycline-inducible plasmids encoding BiP, CNX, CRT, and GRP94 and induced as described in Methods. L444P GC activities are reported in Figure 4a and Figure S3 in Supporting Information. As expected, GC activity was undetectable in untreated cells (cells transfected with empty vector, pcDNA4/TO). BiP overexpression resulted in modest restoration of L444P GC folding (1.4-fold upon induction with 0.2 μg/mL tetracycline for 72 h, Figure S3c in Supporting Information). In order to recapitulate the effect of RyRs blockers and MG-132 cotreatment on BiP upregulation, BiP overexpressing cells were cultured in the presence of MG-132. The combined effect of BiP overexpression (tetracycline 0.2 μg/mL) and MG-132 (0.4 μM) for 48 h resulted in 6.0-fold increase in L444P GC activity with respect to the activity of untreated cells, compared to a 3.3-fold increase in cells treated with MG-132 (Figure 4a). Remarkably, this increase in L444P GC activity corresponds to 75% of wild type GC activity. Overexpression of CNX, CRT, and GRP94 did not result in dramatic increase in L444P GC activity, with the exception of a modest increase in CRT-overexpressing cells (Figure 4a and Figure S3d−l in Supporting Information).

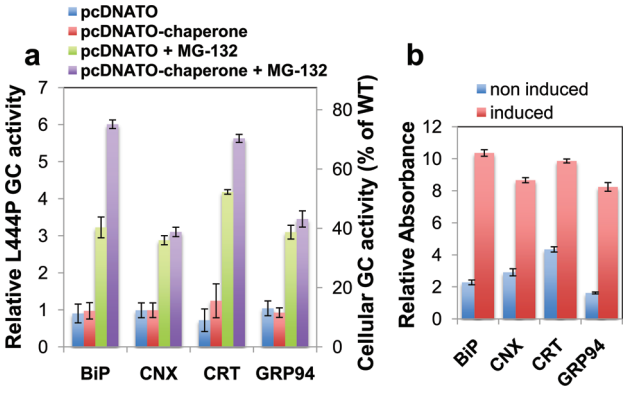

Figure 4. L444P GC activity of patient-derived fibroblasts overexpressing representative ER chaperones and treated with MG-132. (a) Relative L444P GC activities of cells overexpressing ER chaperones (BiP, CNX, CRT, and GRP94, $p < 0.01$) and treated with MG-132 (0.4 μM). Overexpression was induced with media changes with tetracycline-supplemented media 48 h post-transfection, at which times GC enzymatic assays were performed. Relative GC activities were obtained normalizing the activity of cells transfected with empty vector (pcDNA4/TO), cells transfected with empty vector and treated with MG-132, cells transfected with chaperone-encoding plasmid (pcDNA4/TO-chaperone), and cells transfected with chaperone-encoding plasmid and treated with MG-132, by the activity of untreated cells transfected with empty vector. GC activities were obtained as described in Figure 1 and reported as mean ± SD for cells induced with 0.2 μg/mL of tetracycline. (b) Recombinantly expressed chaperone detected by ELISA of induced (0.2 μg/mL tetracycline, 48 h) and noninduced cells. Cell lysates were diluted to 4 mg/mL total protein concentration, incubated in anti-Myc antibody coated plates, and analyzed with chaperone specific antibodies.

Cellular accumulation of Myc-tagged recombinantly expressed chaperones was confirmed by ELISA analyses. Tetracycline induction (0.2 μg/mL) revealed a 3- to 5-fold increase in recombinant protein concentration compared to noninduced cells (Figure 4b and Figure S4 in Supporting Information). Because GC activity assays were conducted by investigating a range of induction conditions (Figure S3 in Supporting Information), this variability in protein accumulation did not hamper our ability to study the effect of different chaperone expression modulation on L444P GC activity.

To further test the hypothesis that BiP expression directly influences the rescue of L444P GC folding, we attempted upregulating chromosomal BiP expression. The Ca^{2+} ionophore A23187 is known to induce BiP promoter (BiP670) at concentrations

dx.doi.org/10.1021/cb100321m |ACS Chem. Biol. 2011, 6, 158–168

that do not induce depletion of cytoplasmic $[Ca^{2+}]$.[48,49] GC activity was evaluated in L444P GC patient-derived fibroblasts cultured with A23187 and/or MG-132 (Figure 5 and Figure S5 in Supporting Information). Co-treatment with A23187 (0.6 μM) and MG-132 (0.4 μM) resulted in a 2.7-fold increase in L444P GC activity, which is higher than what was observed in cells treated with A23187 (1.3-fold) and MG-132 (2.0-fold), confirming that upregulation of BiP expression enhances MG-132-mediated rescue of L444P GC folding.

In summary, we demonstrated that BiP is upregulated in cells treated with MG-132 and particularly with MG-132 and ryanodine (Figure 2a) and that BiP plasmid and chromosomal overexpression enhances MG-132-mediated L444P GC activity increase (Figures 4 and Figure 5). BiP upregulation was previously reported to delay misfolded substrates conformational maturation and ER export through enhanced complex formation with substrate intermediates.[50−52] BiP concentration-dependent ability to increase ER retention was repeatedly observed only for BiP *bona fide* substrates.[53,54] These studies support the notion that increasing BiP expression enhances BiP binding to L444P GC in need for higher chaperoning capacity and longer residence time in the ER. The fact that BiP overexpression does not accelerate substrate folding and ER export is also in agreement with our finding that BiP overexpression or ryanodine treatment alone do not considerably enhance L444P GC activity (Figure 4a and Figure 1a). BiP is an ER lumenal protein whose specific function as promoter of ER folding or ERAD critically depends on a number of interaction partners.[55] Although the question of how BiP plasticity can be channeled for the enhancement of L444P GC folding still remains open, On the basis of the notions that (i) enhanced BiP binding retards substrate conformational maturation but does not promote substrate ERAD and (ii) this effect is only observed for BiP physiologic substrates and thus would not compromise the folding of other proteins, we speculate that BiP function as an ER folding- rather than ERAD-inducing chaperone is to be exploited to effectively rescue the folding of L444P GC. BiP also plays a fundamental role in activating the UPR. Accumulation of misfolded proteins results in BiP release and activation of the three UPR transducers, IRE1, PERK, and ATF6.[40] We suggest that RyRs inhibitor mediated BiP upregulation, as well as plasmid- or chromosome-induced BiP overexpression, by enhancing BiP concentration in the ER, results in increased ER capacity to tolerate increase in misfolded protein without activation of the UPR. This notion is supported by evidence that ryanodine treatment does not induce UPR, as shown by global gene expression analysis (Figure 3 and Table S2 in Supporting Information) and that it ameliorates the cytotoxic effect of MG-132 caused most likely by MG-132-mediated induction of ER stress and UPR, as shown below by analysis of cell toxicity and apoptosis (Table 1).

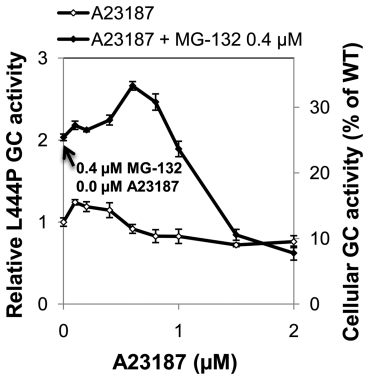

Figure 5. L444P GC activity of patient-derived fibroblasts treated with A23187 and MG-132. Relative L444P GC activities of cells treated with A23187 and MG-132 (0.4 μM) for 48 h ($p < 0.01$). GC activities were obtained as described in Figure 1 and reported as mean ± SD.

Constitutive overexpression of CNX, among ER chaperones, was previously reported to modestly enhance L444P GC proteostasis by increasing the formation of complexes between L444P GC and CNX.[30] Increased binding of CNX to endogenous or overexpressed GC mutants was also previously demonstrated,[5] and the instability of different GC variants, their ER retention, and CNX binding were correlated to their ERAD targeting. As shown herein, L444P GC activity increase is strictly dependent on the chaperone expression level, which was accurately modulated through the use of a tetracycline-inducible plasmid. The study reported herein reveals that CNX mRNA levels were upregulated by small molecule treatment to a lower extent than what was observed for BiP mRNA (Figure 2) and that overexpression of CNX did not significantly increase L444P GC activity (Figure 4b). Our findings, together with previously reported evidence,[5] indicate that CNX is not the key chaperone in the rescue of L444P GC folding.

Table 1. Cell toxicity assay ($p < 0.01$)

		Annexin V		PI	
cell type	cell treatment	population[a]	binding[b]	population[a]	binding[b]
L444P GD	thapsigargin	1.08 ± 0.02	18.01 ± 0.59	5.03 ± 0.32	10.25 ± 0.11
	tunicamycin	−0.05 ± 0.03	19.27 ± 0.19	7.50 ± 0.07	8.20 ± 0.09
	MG-132	−3.38 ± 0.02	43.35 ± 0.31	11.83 ± 0.35	6.98 ± 0.13
	ryanodine	−0.30 ± 0.03	−7.91 ± 0.67	4.70 ± 0.58	−1.57 ± 0.22
	MG-132 + ryanodine	−2.20 ± 0.03	37.21 ± 0.48	9.30 ± 0.53	1.79 ± 0.12
WT	thapsigargin	−9.05 ± 0.10	14.39 ± 0.14	5.65 ± 1.61	21.03 ± 0.41
	tunicamycin	−11.35 ± 0.06	12.98 ± 0.42	7.05 ± 0.69	40.92 ± 0.14
	MG-132	−3.85 ± 0.07	28.34 ± 0.69	2.85 ± 0.32	22.91 ± 0.12
	ryanodine	1.90 ± 0.11	−12.08 ± 1.51	0.90 ± 0.61	−13.32 ± 0.72
	MG-132 + ryanodine	−3.20 ± 0.01	14.92 ± 1.82	1.65 ± 0.03	42.45 ± 0.66

[a] Change (%) in number of cells bound to Annexin V/PI compared to untreated cells. [b] Change (%) in Annexin V/PI binding affinity compared to untreated cells.

Ryanodine Ameliorates Cytotoxicity Induced by Proteostasis Regulation in GD Patient-Derived Cells. Korkotian *et al.* reported that treatment with ryanodine (50 μM) limits the neurotoxic effect of glucosylceramide accumulation and significantly reduces neuronal death.[24] We asked (a) if ryanodine treatment also rescues cytotoxicity caused by glucosylceramide accumulation in L444P GC fibroblasts, (b) if MG-132 treatment by inducing ER stress and UPR causes cytotoxicity and apoptosis, and in that case (c) whether ryanodine treatment limits MG-132-induced cytotoxicity in L444P GC fibroblasts. Small molecules treated cells were tested with the CytoGLO Annexin V-FITC Apoptosis Detection Kit and analyzed by flow cytometry. This assay allows detecting membrane rearrangement (Annexin V binding) and fragmentation (propidium iodide (PI) binding), which normally occur during early and late apoptosis, respectively. As shown in Table 1, Annexin V binding increased 28.34% in wild type fibroblasts treated with MG-132, which was reduced to 14.92% by treatment with ryanodine and MG-132. Thapsigargin (1 μM) and tunicamycin (1 μM) were used as controls as they are known to induce cytotoxicity by activating the UPR[56,57] and resulted in 14.39% and 12.98% increase in Annexin V binding, respectively, compared to untreated cells (Table 1 and Figure S6 in Supporting Information). When the same experiment was conducted using GD fibroblasts carrying L444P GC, Annexin V binding increased 18.01% and 19.27%, respectively, suggesting that L444P GC cells are more susceptible to the cytotoxic effect induced by thapsigargin and tunicamycin treatment than wild type fibroblasts. In L444P GC fibroblasts Annexin V binding increased 43.35% upon MG-132 (0.4 μM) treatment (considerably higher than in wild type fibroblasts), which was also observed to cause an 11.83% increase in cell death (PI binding). However, Annexin V binding decreased 7.91% upon ryanodine (20 μM) treatment, recapitulating the results previously reported using cultures of hippocampal neurons.[24] Treatment with ryanodine and MG-132 caused Annexin V binding to decrease to 37.21% and cell death to increase to 9.30% (Table 1 and Figure S6 in Supporting Information), suggesting that ryanodine alleviates MG-132-induced toxicity and in agreement with the hypothesis that RyRs inhibition recreates a "wild type-like" ER folding environment in L444P GC fibroblasts.

Because one of the key mechanisms of MG-132-mediated rescue of mutated GC folding is UPR induction, we asked whether cell treatment with thapsigargin and tunicamycin could rescue L444P GC folding. A 4- and 2-fold increase in L444P GC were observed in GD cells treated with low concentrations (0.01−1 nM) of thapsigargin and tunicamycin for up to 48 h, an effect that is quickly lost at higher concentrations and longer incubation times (Figure 6), confirming that mild UPR activation promotes mutated GC folding as observed using MG-132.

Cellular $[Ca^{2+}]$ measurements reported recently[30] revealed an increase in $[Ca^{2+}]_{ER}$ and decrease in cytoplasmic $[Ca^{2+}]$ in cells treated with RyRs inhibitors, which supports our conclusion that RyRs blockers restore a "wild type-like" ER environment through modulation of Ca^{2+} homeostasis in L444P GC cells. However, we suggest that careful consideration of small molecule concentrations be used in these studies to avoid misinterpretations of $[Ca^{2+}]$ modulators' ability to influence the folding of mutated L444P GC activity. For instance, contrary to what has been previously reported,[30,58] we show that thapsigargin greatly enhances the folding of L444P GC if used at concentrations (0.01−1 nM) that moderately induce UPR but that are too low

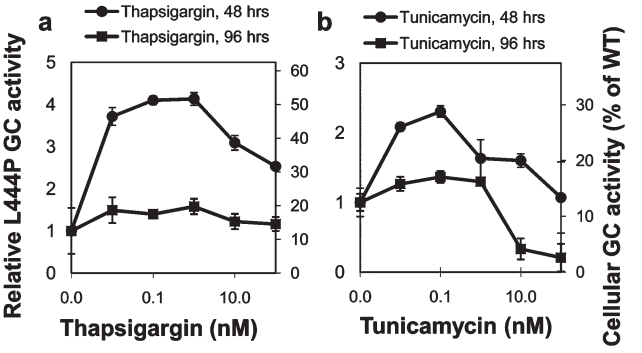

Figure 6. L444P GC activity of patient-derived fibroblasts treated with thapsigargin and tunicamycin. Relative L444P GC activities of cells treated with (a) thapsigargin ($p < 0.01$) and (b) tunicamycin ($p < 0.01$, 48 h; $p < 0.001$, 96 h). GC activities were obtained as described in Figure 1 and reported as mean ± SD.

to have a significant effect on $[Ca^{2+}]_{ER}$ depletion (100 nM[59]) (Figure 6). Cell treatment with considerably higher thapsigargin concentrations (>100 nM) causes $[Ca^{2+}]_{ER}$ depletion, sustained UPR activation, and induction of apoptosis[60,61] and is not compatible with L444P GC folding rescue as previously reported.[30,58]

In summary, results from this study suggest that modulation of Ca^{2+} homeostasis and, particularly, inhibition of excessive $[Ca^{2+}]_{ER}$ synergize with proteostasis regulation to rescue the folding and trafficking of L444P GC in patient-derived fibroblasts. Partial restoration of L444P GC folding is attributed to the function of the main ER chaperone, BiP, and modest upregulation of the UPR. BiP mRNA and protein levels were found to be significantly increased in cells treated with a RyRs blocker (ryanodine) and a proteostasis regulator (MG-132). BiP overexpression and chromosomal induction were shown to enhance MG-132-mediated L444P GC activity. Global gene expression analysis revealed that UPR genes were upregulated by MG-132 treatment, as expected.[16] However, UPR inhibition genes, normally activated as protein homeostasis is restored, were also found to be induced (Figure 3 and Table S2 in Supporting Information). MG-132 seems to partially restore L444P GC folding by inducing short pulses of UPR or possibly to moderate UPR activation, which is likely to promote folding of this destabilized GC variant without disruptive effects on native protein homeostasis. Gene expression analysis also revealed that ryanodine-mediated RyRs inhibition does not directly induce heat-shock stress and UPR but slightly enhances or attenuates MG-132-induced modulation of key genes of the proteostasis network, thereby boosting the folding-promoting activity of MG-132 (Figure 3). In addition, RyRs inhibition partially rescues GD cells from MG-132-induced cytotoxicity and apoptosis induction (Table 1). These results (i) strengthen our hypothesis that RyRs inhibition counteracts the deleterious effect of substrate accumulation on Ca^{2+} homeostasis and reinstates a "wild type-like" folding environment in L444P GC fibroblasts and (ii) underscore the value of RyRs blockers as research tools to investigate proteostasis modulation in GD cells.

METHODS

Reagents, Cell Lines, and Media. Celastrol and MG-132 were purchased from Alexis Biochemicals. Conduritol B Epoxide (CBE) was from Toronto Research Chemicals. 4-Methylumbelliferyl β-D-glucoside

dx.doi.org/10.1021/cb100321m |*ACS Chem. Biol.* 2011, 6, 158–168

(MUG) was from Sigma, and dantrolene and ryanodine were from Tocris Bioscience. Bovine serum albumin was from Jackson ImmunoResearch Laboratories. Cell culture media were purchased from Gibco. Lipofectamine 2000 was from Invitrogen, and the TMB Reagent set was from BioLegend.

Gaucher's disease patient-derived primary fibroblasts for WT (GM00498) and homozygous for the L444P (1448T > C) mutation (GM10915) were obtained from Coriell Cell Repositories. Fibroblasts were grown in minimal essential medium with Earle's salts supplemented with 10% heat-inactivated fetal bovine serum and 1% glutamine Pen-Strep at 37 °C in 5% CO_2. Cell medium was replaced every 3 or 4 days. Monolayers were passaged upon reaching confluency with TrypLE Express.

Cloning and Transfection Procedures. The human cDNA clones of BiP (P11021), Calnexin (P27824), Calreticulin (P15253), and Grp94 (P14625) were obtained from Origene and cloned into pcDNA4/TO (Invitrogen). cDNA sequences were amplified by PCR using the primers reported in Table S1 in Supporting Information, adding the myc tag (N-EQKLISEEDL-C) at the 3′ end of each sequence. PCR products were digested with the appropriate restriction enzymes (Table S1) and ligated into the inducible expression vector pcDNA4/TO digested likewise. Plasmid sequences were confirmed by automated sequencing.

Transfection procedures were performed as described: briefly, 10^4 cells in 100 μL of growth medium were plated in each well of 96-well plates. Transfection reactions were performed when cells reached 70−80% confluency (~24 h after plating) using Lipofectamine 2000 in medium with serum and without antibiotics. Tetracycline was added to the medium 24 h post-transfection at concentrations ranging from 0 to 1.5 μg/mL, and lysosomal GC activity was measured after 24, 48, and 72 h.

Glucocerebrosidase (GC) Activity Assay. The intact cell GC activity assay was conducted as previously described.[16] Cells (10^4) were plated in each well of a 96-well plate (100 μL per well) and incubated overnight to allow cell attachment. Fresh medium containing small molecules was replaced, and plates were incubated at 37 °C (the time of incubation is specified in each experiment). The medium was then removed, and monolayers were washed with PBS. The assay reaction was started by the addition of 50 μL of 2.5 mM MUG in 0.2 M acetate buffer (pH 4.0) to each well. Plates were incubated at 37 °C for 7 h, and the reaction was stopped by the addition of 150 μL of 0.2 M glycine buffer (pH 10.8) to each well. Liberated 4-methylumbelliferone was measured (excitation 365 nm, emission 445 nm) with a SpectraMax Gemini plate reader (Molecular Device). Control experiments to evaluate the extent of unspecific non-lysosomal GC activity were performed by adding CBE to a final concentration of 1 mM. The measured GC activities were normalized to the activity of untreated cells.

Quantitative RT-PCR. RT-PCR was conducted as previously described.[16] Briefly, total RNA was extracted using RNeasy Mini Kit (Qiagen). cDNA was synthesized from total RNA using Reverse Transcription Kit (Invitrogen). After reverse transcription, total cDNA amount was measured using a NanoDrop 2000 (Thermo Scientific). Quantitative PCR reactions were performed using 200 ng/μL cDNA, QuantiTect SYBR Green PCR Kit (Applied Biosystems), and corresponding primers (Table S1 in Supporting Information) in the ABI PRISM 7900 system (Applied Biosystems). Samples were heated for 15 min at 95 °C and amplified in 45 cycles of 15 s at 94 °C, 30 s at 57 °C, and 30 s at 72 °C. Analysis was done using SDS2.1 software (Applied Biosystems). Threshold cycle (C_T) was extracted from the PCR amplification plot. The ΔC_T value was used to describe the difference between the C_T of a target gene and the C_T of the housekeeping gene, GAPDH: $\Delta C_T = C_T$ (target gene) − C_T (GAPDH). The relative mRNA expression level of a target gene of drug-treated cells was normalized to that of untreated cells: relative mRNA expression level = $2 \exp[-(\Delta C_T$ (treated cells) − ΔC_T (untreated cells))]. Each data point was evaluated in triplicate and measured three times.

Illumina Chip Analyses. Cells were treated with small molecules for 24 h at 37 °C before total RNA was extracted. Two hundred nanograms of Total RNA were amplified and purified using Illumina TotalPrep RNA Amplification Kit (Ambion) following kit instructions. Briefly, first strand cDNA was synthesized by incubating RNA with T7 oligo(dT) primer and reverse transcriptase mix at 42 °C for 2 h. RNase H and DNA polymerase master mix were immediately added into the reaction mix following reverse transcription and were incubated for 2 h at 16 °C to synthesize second strand cDNA. RNA, primers, enzymes, and salts that would inhibit *in vitro* transcription were removed through cDNA filter cartridges (part of the amplification kit). *In vitro* transcription was performed and biotinylated cRNA was synthesized by 14-h amplification with dNTP mix containing biotin-dUTP and T7 RNA polymerase. Amplified cRNA was subsequently purified and concentration was measured by NanoDrop ND-1000 Spectrophotometer (NanoDrop Technologies). An aliquot of 750 nanograms of amplified products was loaded onto Illumina Sentrix Beadchip Array Human-8 arrays, hybridized at 58 °C in an Illumina Hybridization Oven (Illumina) for 17 h, washed and incubated with straptavidin-Cy3 to detect biotin-labeled cRNA on the arrays. Arrays were dried and scanned with BeadArray Reader (Illumina). Data were analyzed using BeadStudio software (Illumina). Clustering and pathway analysis were performed with GenomeStudio and Ingenuity Pathway Analysis (Ingenuity Systems, Inc.) softwares, respectively.

Immunocytochemistry Studies. Cells were lysated with the complete lysis-M buffer containing a protease inhibitor cocktail (Roche) following manufacturer's instructions. Total cell protein was determined by Bradford assay (Pierce), and each sample was diluted to the same protein concentration. Because a Myc tag was fused to the C-terminus of BiP, CNX, CRT, and GRP94, ELISA experiments were conducted using an anti-Myc antibody to capture only recombinantly expressed proteins, and chaperone-specific antibodies for detection. 96-well ELISA plates (BD) were coated with 100 μL/well of 1 μg/mL capturing Myc tag antibody (Abcam) in 0.1 M sodium bicarbonate. Following overnight incubation at 4 °C, plates were washed with PBS/0.1% Tween-20, and incubated with 200 μL/well of blocking buffer containing 0.01 g/mL BSA in PBS overnight at 4 °C. Plates were washed, and 100 μL of PBS containing 1 mg/mL BSA was added to each well. Then, 100 μL of antigen was added to the first column and serial dilutions were obtained by transferring 100 μL across the plate. Negative controls were included that did not contain antigen. Plates were incubated for 4 h at RT. After additional washes, plates were incubated for 2 h at RT with primary antibodies (rabbit anti-BiP, rabbit anti-CNX, and mouse anti-CRT (Stressgen), rabbit anti-GRP94 (Santa Cruz Biotechnology)), and subsequently with secondary antibodies (HRP conjugated goat anti-rabbit (Santa Cruz Biotechnology) or goat anti-mouse IgG (Stressgen)) for 1 h. TMB substrate reagent was used to detect antibody binding according to the manufacturer's procedures.

Western blot analyses were performed as previously described.[16] Aliquots of cell lysates were separated in a 10% SDS-PAGE gel, and Western blot analyses were performed using rabbit anti-GC (Sigma-Aldrich) or rabbit anti-GAPDH (Santa Cruz Biotechnology) and goat anti-rabbit HRP-conjugated antibody as secondary antibody. Blots were visualized using SuperSignal West Femto Maximum (Pierce), and bands were quantified by NIH Java Image analysis software.

Toxicity Assay. Wild type and L444P GC patient-derived fibroblasts were treated with MG-132 (0.4 μM), ryanodine (20 μM), thapsigargin (1 μM), and tunicamycin (1 μM) for 16 h at 37 °C. Cells were collected and cell toxicity tested with the CytoGLO Annexin V-FITC Apoptosis Detection Kit (IMGENEX) according to the manufacturer's instructions and analyzed by flow cytometry (FACSCanto II, Beckon Dickingson) with a 488-nm argon laser.

Statistical Analysis. All data is presented as mean ± SD, and statistical significance was calculated using a two-tailed *t*-test.

■ ASSOCIATED CONTENT

Supporting Information. This material is available free of charge via the Internet at http://pubs.acs.org.

■ AUTHOR INFORMATION

Corresponding Author
*segatori@rice.edu.

■ REFERENCES

(1) Futerman, A. H., and van Meer, G. (2004) The cell biology of lysosomal storage disorders. *Nat. Rev. Mol. Cell Biol.5*, 554–565.

(2) Schueler, U. H., Kolter, T., Kaneski, C. R., Zirzow, G. C., Sandhoff, K., and Brady, R. O. (2004) Correlation between enzyme activity and substrate storage in a cell culture model system for Gaucher disease. *J. Inherited Metab. Dis.27*, 649–658.

(3) Hruska, K. S., LaMarca, M. E., Scott, C. R., and Sidransky, E. (2008) Gaucher disease: mutation and polymorphism spectrum in the glucocerebrosidase gene (GBA). *Hum. Mutat.29*, 567–583.

(4) Schmitz, M., Alfalah, M., Aerts, J. M., Naim, H. Y., and Zimmer, K. P. (2005) Impaired trafficking of mutants of lysosomal glucocerebrosidase in Gaucher's disease. *Int. J. Biochem. Cell Biol.37*, 2310–2320.

(5) Ron, I., and Horowitz, M. (2005) ER retention and degradation as the molecular basis underlying Gaucher disease heterogeneity. *Hum. Mol. Genet.14*, 2387–2398.

(6) Desnick, R. J., and Schuchman, E. H. (2002) Enzyme replacement and enhancement therapies: lessons from lysosomal disorders. *Nat. Rev. Genet.3*, 954–966.

(7) Futerman, A. H., Sussman, J. L., Horowitz, M., Silman, I., and Zimran, A. (2004) New directions in the treatment of Gaucher disease. *Trends Pharmacol. Sci.25*, 147–151.

(8) Elstein, D., and Zimran, A. (2009) Review of the safety and efficacy of imiglucerase treatment of Gaucher disease. *Biologics3*, 407–417.

(9) Ficicioglu, C. (2008) Review of miglustat for clinical management in Gaucher disease type 1. *Ther. Clin. Risk Manage.4*, 425–431.

(10) Grabowski, G. A. (1997) Gaucher disease: gene frequencies and genotype/phenotype correlations. *Genet. Test.1*, 5–12.

(11) Dvir, H., Harel, M., McCarthy, A. A., Toker, L., Silman, I., Futerman, A. H., and Sussman, J. L. (2003) X-ray structure of human acid-beta-glucosidase, the defective enzyme in Gaucher disease. *EMBO Rep.4*, 704–709.

(12) Grace, M. E., Newman, K. M., Scheinker, V., Berg-Fussman, A., and Grabowski, G. A. (1994) Analysis of human acid beta-glucosidase by site-directed mutagenesis and heterologous expression. *J. Biol. Chem. 269*, 2283–2291.

(13) Sawkar, A. R., Schmitz, M., Zimmer, K. P., Reczek, D., Edmunds, T., Balch, W. E., and Kelly, J. W. (2006) Chemical chaperones and permissive temperatures alter localization of Gaucher disease associated glucocerebrosidase variants. *ACS Chem. Biol.1*, 235–251.

(14) Sawkar, A. R., Cheng, W. C., Beutler, E., Wong, C. H., Balch, W. E., and Kelly, J. W. (2002) Chemical chaperones increase the cellular activity of N370S beta-glucosidase: a therapeutic strategy for Gaucher disease. *Proc. Natl. Acad. Sci. U.S.A.99*, 15428–15433.

(15) Balch, W. E., Morimoto, R. I., Dillin, A., and Kelly, J. W. (2008) Adapting proteostasis for disease intervention. *Science319*, 916–919.

(16) Mu, T. W., Ong, D. S., Wang, Y. J., Balch, W. E., Yates, J. R.3rd, Segatori, L., and Kelly, J. W. (2008) Chemical and biological approaches synergize to ameliorate protein-folding diseases. *Cell134*, 769–781.

(17) Jonsson, L. M., Murray, G. J., Sorrell, S. H., Strijland, A., Aerts, J. F., Ginns, E. I., Barranger, J. A., Tager, J. M., and Schram, A. W. (1987) Biosynthesis and maturation of glucocerebrosidase in Gaucher fibroblasts. *Eur. J. Biochem.164*, 171–179.

(18) Beutler, E., Kuhl, W., and Sorge, J. (1984) Cross-reacting material in Gaucher disease fibroblasts. *Proc. Natl. Acad. Sci. U.S.A.81*, 6506–6510.

(19) Michelakakis, H., Dimitriou, E., Van Weely, S., Boot, R. G., Mavridou, I., Verhoek, M., and Aerts, J. M. (1995) Characterization of glucocerebrosidase in Greek Gaucher disease patients: mutation analysis and biochemical studies. *J. Inherited Metab. Dis.18*, 609–615.

(20) Meivar-Levy, I., Horowitz, M., and Futerman, A. H. (1994) Analysis of glucocerebrosidase activity using *N*-(1-[14C]hexanoyl)-D-erythroglucosylsphingosine demonstrates a correlation between levels of residual enzyme activity and the type of Gaucher disease. *Biochem. J.303* (Pt 2), 377–382.

(21) Bodamer, O. A., and Hung, C. Laboratory and genetic evaluation of Gaucher disease, *Wien Med. Wochenschr.*Epub ahead of print August 16, 2010; DOI: 10.1007/s10354-010-0814-1.

(22) Michalak, M., Robert Parker, J. M., and Opas, M. (2002) Ca2+ signaling and calcium binding chaperones of the endoplasmic reticulum. *Cell Calcium32*, 269–278.

(23) Baumann, O., and Walz, B. (2001) Endoplasmic reticulum of animal cells and its organization into structural and functional domains. *Int. Rev. Cytol.205*, 149–214.

(24) Korkotian, E., Schwarz, A., Pelled, D., Schwarzmann, G., Segal, M., and Futerman, A. H. (1999) Elevation of intracellular glucosylceramide levels results in an increase in endoplasmic reticulum density and in functional calcium stores in cultured neurons. *J. Biol. Chem.274*, 21673–21678.

(25) Lloyd-Evans, E., Pelled, D., Riebeling, C., Bodennec, J., de-Morgan, A., Waller, H., Schiffmann, R., and Futerman, A. H. (2003) Glucosylceramide and glucosylsphingosine modulate calcium mobilization from brain microsomes via different mechanisms. *J. Biol. Chem.278*, 23594–23599.

(26) Pelled, D., Trajkovic-Bodennec, S., Lloyd-Evans, E., Sidransky, E., Schiffmann, R., and Futerman, A. H. (2005) Enhanced calcium release in the acute neuronopathic form of Gaucher disease. *Neurobiol. Dis.18*, 83–88.

(27) Pelled, D., Lloyd-Evans, E., Riebeling, C., Jeyakumar, M., Platt, F. M., and Futerman, A. H. (2003) Inhibition of calcium uptake via the sarco/endoplasmic reticulum Ca2+-ATPase in a mouse model of Sandhoff disease and prevention by treatment with *N*-butyldeoxynojirimycin. *J. Biol. Chem.278*, 29496–29501.

(28) Ginzburg, L., and Futerman, A. H. (2005) Defective calcium homeostasis in the cerebellum in a mouse model of Niemann-Pick A disease. *J. Neurochem.95*, 1619–1628.

(29) Lloyd-Evans, E., Morgan, A. J., He, X., Smith, D. A., Elliot-Smith, E., Sillence, D. J., Churchill, G. C., Schuchman, E. H., Galione, A., and Platt, F. M. (2008) Niemann-Pick disease type C1 is a sphingosine storage disease that causes deregulation of lysosomal calcium. *Nat. Med.14*, 1247–1255.

(30) Ong, D. S., Mu, T. W., Palmer, A. E., and Kelly, J. W. (2010) Endoplasmic reticulum Ca2+ increases enhance mutant glucocerebrosidase proteostasis. *Nat. Chem. Biol.6*, 424–432.

(31) Buck, E., Zimanyi, I., Abramson, J. J., and Pessah, I. N. (1992) Ryanodine stabilizes multiple conformational states of the skeletal muscle calcium release channel. *J. Biol. Chem.267*, 23560–23567.

(32) Nagasaki, K., and Fleischer, S. (1988) Ryanodine sensitivity of the calcium release channel of sarcoplasmic reticulum. *Cell Calcium9*, 1–7.

(33) Ward, A., Chaffman, M. O., and Sorkin, E. M. (1986) Dantrolene. A review of its pharmacodynamic and pharmacokinetic properties and therapeutic use in malignant hyperthermia, the neuroleptic malignant syndrome and an update of its use in muscle spasticity. *Drugs32*, 130–168.

(34) Kang, J. J., Hsu, K. S., and Lin-Shiau, S. Y. (1994) Effects of bipyridylium compounds on calcium release from triadic vesicles isolated from rabbit skeletal muscle. *Br. J. Pharmacol.112*, 1216–1222.

(35) Maley, F., Trimble, R. B., Tarentino, A. L., and Plummer, T. H. Jr. (1989) Characterization of glycoproteins and their associated oligosaccharides through the use of endoglycosidases. *Anal. Biochem.180*, 195–204.

(36) Platt, F. M., Jeyakumar, M., Andersson, U., Priestman, D. A., Dwek, R. A., Butters, T. D., Cox, T. M., Lachmann, R. H., Hollak, C., Aerts, J. M., Van Weely, S., Hrebicek, M., Moyses, C., Gow, I., Elstein, D., and Zimran, A. (2001) Inhibition of substrate synthesis as a strategy for glycolipid lysosomal storage disease therapy. *J. Inherited Metab. Dis.24*, 275–290.

(37) Brumshtein, B., Greenblatt, H. M., Butters, T. D., Shaaltiel, Y., Aviezer, D., Silman, I., Futerman, A. H., and Sussman, J. L. (2007) Crystal structures of complexes of *N*-butyl- and *N*-nonyl-deoxynojirimycin bound to acid beta-glucosidase: insights into the mechanism of chemical chaperone action in Gaucher disease. *J. Biol. Chem.282*, 29052–29058.

(38) Kleizen, B., and Braakman, I. (2004) Protein folding and quality control in the endoplasmic reticulum. *Curr. Opin. Cell. Biol.16*, 343–349.

(39) Fill, M., and Copello, J. A. (2002) Ryanodine receptor calcium release channels. *Physiol. Rev.82*, 893–922.

(40) Ron, D., and Walter, P. (2007) Signal integration in the endoplasmic reticulum unfolded protein response. *Nat. Rev. Mol. Cell Biol.8*, 519–529.

(41) Perkins, K. J., Byers, S., Yogalingam, G., Weber, B., and Hopwood, J. J. (1999) Expression and characterization of wild type and mutant recombinant human sulfamidase. Implications for Sanfilippo (Mucopolysaccharidosis IIIA) syndrome. *J. Biol. Chem.274*, 37193–37199.

(42) Schroder, M., and Kaufman, R. J. (2005) The mammalian unfolded protein response. *Annu. Rev. Biochem.74*, 739–789.

(43) Lee, A. H., Iwakoshi, N. N., and Glimcher, L. H. (2003) XBP-1 regulates a subset of endoplasmic reticulum resident chaperone genes in the unfolded protein response. *Mol. Cell. Biol.23*, 7448–7459.

(44) Scorrano, L., Oakes, S. A., Opferman, J. T., Cheng, E. H., Sorcinelli, M. D., Pozzan, T., and Korsmeyer, S. J. (2003) BAX and BAK regulation of endoplasmic reticulum Ca2+: a control point for apoptosis. *Science300*, 135–139.

(45) Urano, F., Wang, X., Bertolotti, A., Zhang, Y., Chung, P., Harding, H. P., and Ron, D. (2000) Coupling of stress in the ER to activation of JNK protein kinases by transmembrane protein kinase IRE1. *Science287*, 664–666.

(46) Travers, K. J., Patil, C. K., Wodicka, L., Lockhart, D. J., Weissman, J. S., and Walter, P. (2000) Functional and genomic analyses reveal an essential coordination between the unfolded protein response and ER-associated degradation. *Cell101*, 249–258.

(47) Wang, J., and Best, P. M. (1992) Inactivation of the sarcoplasmic reticulum calcium channel by protein kinase. *Nature359*, 739–741.

(48) Drummond, I. A., Lee, A. S., Resendez, E.Jr., and Steinhardt, R. A. (1987) Depletion of intracellular calcium stores by calcium ionophore A23187 induces the genes for glucose-regulated proteins in hamster fibroblasts. *J. Biol. Chem.262*, 12801–12805.

(49) Chao, C. C., and Lin-Chao, S. (1992) A direct-repeat sequence of the human BiP gene is required for A23187-mediated inducibility and an inducible nuclear factor binding. *Nucleic Acids Res.20*, 6481–6485.

(50) Muresan, Z., and Arvan, P. (1998) Enhanced binding to the molecular chaperone BiP slows thyroglobulin export from the endoplasmic reticulum. *Mol. Endocrinol.12*, 458–467.

(51) Gorbatyuk, M. S., Knox, T., LaVail, M. M., Gorbatyuk, O. S., Noorwez, S. M., Hauswirth, W. W., Lin, J. H., Muzyczka, N., and Lewin, A. S. (2010) Restoration of visual function in P23H rhodopsin transgenic rats by gene delivery of BiP/Grp78. *Proc. Natl. Acad. Sci. U.S.A.107*, 5961–5966.

(52) Xu, P., and Robinson, A. S. (2009) Decreased secretion and unfolded protein response up-regulation are correlated with intracellular retention for single-chain antibody variants produced in yeast. *Biotechnol. Bioeng.104*, 20–29.

(53) Dorner, A. J., and Kaufman, R. J. (1994) The levels of endoplasmic reticulum proteins and ATP affect folding and secretion of selective proteins. *Biologicals22*, 103–112.

(54) Dorner, A. J., Wasley, L. C., and Kaufman, R. J. (1992) Overexpression of GRP78 mitigates stress induction of glucose regulated proteins and blocks secretion of selective proteins in Chinese hamster ovary cells. *EMBO J.11*, 1563–1571.

(55) Vembar, S. S., Jonikas, M. C., Hendershot, L. M., Weissman, J. S., and Brodsky, J. L. (2010) J domain co-chaperone specificity defines the role of BIP during protein translocation. *J. Biol. Chem.285*, 22484–22494.

(56) Duksin, D., and Bornstein, P. (1977) Changes in surface properties of normal and transformed cells caused by tunicamycin, an inhibitor of protein glycosylation. *Proc. Natl. Acad. Sci. U.S.A.74*, 3433–3437.

(57) Chen, L. H., Jiang, C. C., Kiejda, K. A., Wang, Y. F., Thorne, R. F., Zhang, X. D., and Hersey, P. (2007) Thapsigargin sensitizes human melanoma cells to TRAIL-induced apoptosis by up-regulation of TRAIL-R2 through the unfolded protein response. *Carcinogenesis28*, 2328–2336.

(58) Mu, T. W., Fowler, D. M., and Kelly, J. W. (2008) Partial restoration of mutant enzyme homeostasis in three distinct lysosomal storage disease cell lines by altering calcium homeostasis. *PLoS Biol.6*, No. e26.

(59) Yoshida, I., Monji, A., Tashiro, K.-i., Nakamura, K.-i., Inoue, R., and Kanba, S. (2006) Depletion of intracellular Ca2+ store itself may be a major factor in thapsigargin-induced ER stress and apoptosis in PC12 cells. *Neurochem. Int.48*, 696–702.

(60) Futami, T., Miyagishi, M., and Taira, K. (2005) Identification of a network involved in thapsigargin-induced apoptosis using a library of small interfering RNA expression vectors. *J. Biol. Chem.280*, 826–831.

(61) Jin, T., Nakatani, H., Taguchi, T., Sonobe, H., Morimoto, N., Sugimoto, T., Akimori, T., Nakano, T., Namikawa, T., Okabayashi, T., Kobayashi, M., and Araki, K. (2006) Thapsigargin enhances cell death in the gastrointestinal stromal tumor cell line, GIST-T1, by treatment with Imatinib (Glivec). *J. Health Sci.52*, 110–117.